Astron. Astrophys. 345, 583–591 (1999)

ASTRONOMY
AND
ASTROPHYSICS

An extremely X-ray luminous proto–Herbig Ae/Be star in the Serpens star forming region*

Thomas Preibisch[1,2]

[1] Max-Planck-Institut für Radioastronomie, Auf dem Hügel 69, D-95121 Bonn, Germany
[2] Astronomisches Institut, Universität Würzburg, Am Hubland, D-97074 Würzburg, Germany

Received 16 November 1998 / Accepted 2 March 1999

Abstract. We present near-infrared spectra for the highly obscured, optically invisible young stellar object EC 95 in the Serpens molecular cloud, from which we recently could detect strong X-ray emission with ROSAT. Its location in the HR diagram suggests this object to be an extremely young ($\sim 2\times10^5$ yr old) intermediate-mass ($\sim 4\ M_\odot$) star, which is most likely the progenitor of a B-type or early A-type main sequence star. The only reasonable explanation for its extremely strong X-ray emission ($L_X \sim 1.2 \times 10^{33}$ erg/sec) seems to be coronal, i.e. magnetic activity; this view is also supported by the strong radio emission of EC 95. This is quite surprising, since one usually does not expect a magnetic field on intermediate-mass stars, which are thought to lack surface convection zones, the prerequisite for a solar-like dynamo effect. A possible explanation might be that EC 95 currently goes through a short period of deuterium shell burning, which causes convection near the stellar surface and might give rise to a dynamo effect and a corona.

Key words: stars: coronae – stars: individual: EC 95: J182958+011247 – stars: individual: EC 95: J182958+011252 – stars: magnetic fields – stars: pre-main sequence – X-rays: stars

1. Introduction

The Serpens dark cloud is one of the most active nearby star forming regions (for a review see Eiroa 1991). It contains numerous young stellar objects (YSOs) in all stages of evolution, from infrared class 0 protostars to infrared class III T Tauri stars (see Lada 1987 for the infrared classification scheme of YSOs). Many of these YSOs are highly obscured and therefore optically invisible. Recent near infrared (NIR) surveys of the Serpens cloud by Eiroa & Casali (1992) and Giovannetti et al. (1998) have led to the detection of more than 150 NIR sources. The distance estimates for the Serpens cloud found in the literature range from 250 pc to 700 pc (see Eiroa 1991). De Lara et al. (1991) derived $d \sim 310$ pc from extinction measurements of several stars. Hogerheijde et al. (1999) argue that a distance of 400 pc might be more appropriate, but in order to be conservative we decided to use 310 pc for this work.

In their pioneering NIR observations of the Serpens cloud, Strom et al. (1976) detected an optically invisible infrared source a few arcminutes south of the Serpens Reflection Nebula. This object, called SVS 4, could later be resolved into a small cluster of at least 11 individual NIR sources by Eiroa & Casali (1989) and constitutes one of the densest clusterings of YSOs know. In a deep ROSAT HRI study of the Serpens star forming region, Preibisch (1998; P98 hereafter) could detect X-ray emission from a point source in SVS 4. The X-ray source position coincides within $2''$ with the infrared source EC 95 (cf. Eiroa & Casali 1992), but the X-ray error box also contains the nearby source EC 92. Most probably, EC 95 is the counterpart of the X-ray source, but it cannot be fully excluded that EC 92 might be related to the X-ray source. In any way, considering the very high extinction of these objects ($A_V \approx 25$–35 mag), the X-ray luminosity of this source must be about 10^{33} erg/sec in the 0.1–2.4 keV ROSAT band, making it the most X-ray luminous YSO in terms of non-flaring, quiescent X-ray emission ever detected.

Besides NIR photometric data, virtually nothing was known about the individual stars in SVS 4 until now. In order to obtain more information about the nature and the evolutionary status of this extraordinary X-ray source, we have performed infrared spectroscopy of EC 92 and EC 95 and analyzed further observations of the SVS 4 region.

2. UKIRT near-infrared spectroscopy

2.1. Observations and data analysis

In the night of 24 June 1998, K- and H-band spectra of EC 95 and EC 92 were obtained for us as a part of the UKIRT Service Programme. The observations were performed with CGS4, a $1-5\ \mu$m multi-purpose 2D grating spectrometer containing a 256×256 InSb array, using the 40 l/mm grating. The $0.61''$ wide slit was oriented 7° west of north, to include both objects. The bright F5V star BS6797 was observed as a calibration star for atmospheric correction. Data were taken in a normal stare and

Send offprint requests to: Thomas Preibisch
(preib@astro.uni-wuerzburg.de)

* Mainly based on observations collected at the United Kingdom Infrared Telescope, Hawaii, USA

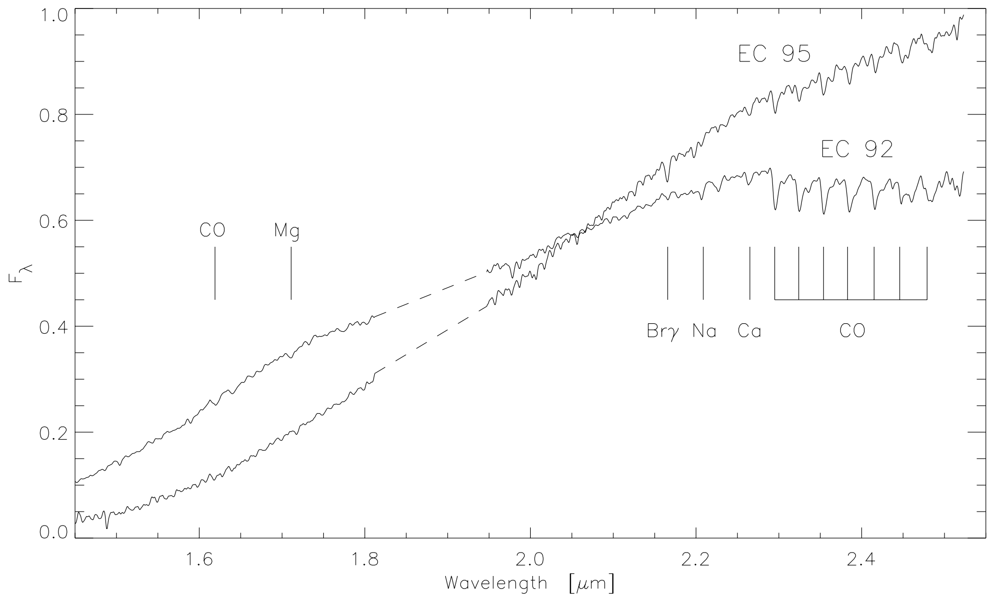

Fig. 1. This plot shows the UKIRT H- and K-band spectra of EC 95 and EC 92. The positions of important lines are marked. The 1.8–1.95 μm range is skipped and interpolated by the dashed lines, since it contains many strong atmospheric absorptions lines which blend with the hydrogen absorption lines of the calibration star, making atmospheric correction very difficult.

nod-along-the-slit mode. The total exposure times were 480 sec for the K-band spectrum, and 1080 sec for the H-band spectrum. An Argon lamp spectrum was used for wavelength calibration.

Data reduction was performed with IRAF[1]. After differencing the object and sky frames, we extracted the positive and negative spectra, and then co-added all spectra of each star. In order to remove the instrumental and atmospheric features in the spectra, we divided the object spectra by the spectrum of the calibration star, from which we had removed the H I absorption lines. Finally, the resulting spectra were multiplied by a Planck function at a blackbody temperature equal to that of the calibration star. The features and shape of the final spectra should be representative of the true object spectrum. For further details on NIR spectral data reduction we refer to Greene & Lada (1996).

The resulting spectra are shown in Fig. 1. The effective resolution is $R \sim 750$ in the K-band and $R \sim 550$ in the H-band, the signal to noise ratio of the spectra is ~ 50. Several atomic and CO absorption lines can be seen in the spectra and clearly show that both objects are late type stars[2]. The spectra do not show any of the emission lines found in some YSOs.

2.2. Determination of spectral types and stellar parameters

We have used the measured line widths summarized in Table 1 and published photometric data ($J, H, K = 16.7, 12.3, 9.8$ for EC 95, $J, H, K = 15.4, 12.0, 10.2$ for EC 92; Giovannetti et al. 1998) to determine spectral type and surface gravity with the method presented by Greene & Meyer (1995; GM95 hereafter). The location of the stars in the diagram of atomic versus CO indices is shown in Fig. 2, where we also show the calibration lines from GM95 for stars of luminosity class V and III. One cannot directly derive the spectral type from the position in this diagram, since one has to take into account spectral continuum veiling, which is caused by the excess emission from hot circumstellar matter and will decrease the line widths. In order to correct for this veiling, we used the iterative procedure described by GM95, to find a self-consistent set of the stellar parameters spectral type, extinction, and veiling. For any details of this method we refer to GM95. We assumed the veiling to be significant in the K-band only, what can be justified by the very modest NIR excesses of these stars as inferred from their positions in the color-color diagram, and used the reddening relations $A_V = 9.37\ E(J-H) = 3.55\ A_J = 16.25\ E(H-K) = 8.93\ A_K$ (cf. Rieke & Lebofsky 1985).

For EC 95, the uncorrected line widths suggest a spectral type of ∼K1. After two iteration steps we find a stable solution with spectral type K2, $r_k = 0.16$, and $A_V = 36.5$ mag. For EC 92 the uncorrected line widths suggest a spectral type of ∼K4, and after three iteration steps the procedure converges at spectral type M0, $r_k = 0.4$, and $A_V = 27.2$ mag. Finally, we compute the luminosity of the stars from their dereddened J-band magnitudes, using the BC_J bolometric correction from Hartigan et al. (1994). All stellar parameters and the corresponding uncertainties are summarized in Table 2.

Table 1. Equivalent widths of absorption lines in the K-band spectra. The uncertainties of the measurements are about 10%.

line	Na	Ca	CO [0-2]	CO [2-4]
λ [μm]	2.21	2.26	2.29	2.35
EW(EC 95) [Å]	1.1	1.6	2.8	2.6
EW(EC 92) [Å]	1.8	2.4	7.6	7.7

[1] IRAF is distributed by the National Optical Astronomy Observatories, which are operated by the Association of Universities for Research in Astronomy, Inc., under cooperative agreement with the National Science Foundation.

[2] This result also excludes the unlikely, but not absolutely impossible case that we are dealing with an extragalactic object (e.g. a quasar) behind the star forming region.

Table 2. Stellar parameters for EC 95 and 92. Masses are listed individually for each set of PMS tracks (S97: Siess et al. 1997; DM94: D'Antona & Mazzitelli 1994; S94: Swenson et al. 1994; I65: Iben 1965; PS93: Palla & Stahler 1993); the first value gives the best estimate, the values in square brackets give the range of masses permitted by the uncertainties.

	EC 95		EC 92
SpT	K0 – K4		K7 – M2
$L_\star$ $[L_\odot]$	60^{+30}_{-20}		8^{+4}_{-3}
r_k	0.16 ± 0.05		0.4 ± 0.1
A_J [mag]	10.3 ± 0.2		7.7 ± 0.2
A_V [mag]	36 ± 2		27 ± 2
$R_\star$ $[R_\odot]$	10.3 ± 3.5		6.5 ± 2.2
age [yr]	$2^{+2}_{-1} \times 10^5$		$\lesssim 10^5$
mass $[M_\odot]$ S97	4	[2.2–4.5]	< 0.7
mass $[M_\odot]$ DM94	> 2.5	$[> 1.5]$	≈ 0.2–0.5
mass $[M_\odot]$ S94	~ 3	$[> 1.6]$	≈ 0.2–0.7
mass $[M_\odot]$ I65	~ 3.5	[3.0–4.0]	
mass $[M_\odot]$ PS93	≈ 4	$[\approx 3$–4.5]	≈ 0.3–0.8

A comparison with the extinction and luminosity estimates derived by P98, which were based on the photometric data only, shows good agreement for EC 92 and also for the extinction of EC 95. The stellar luminosity for EC 95 we find here ($60\,L_\odot$) is about a factor of 2 higher than the previous estimate by P98 ($\approx 26\,L_\odot$). This difference is caused by the bolometric method which had to be used by P98, because there was no spectral information available at that time. This bolometric method (cf. Greene et al. 1994; Eq. 2) is valid for M-type stars, but seriously underestimates the luminosities for spectral types earlier than ∼K5. The new luminosity derived here is much more reliable, since it is based on a proper bolometric correction for the K2 spectral type of EC 95.

For EC 95 our data suggest a surface gravity slightly above that for luminosity class V stars; the veiling is typical for objects of infrared class II or III (cf. Greene & Lada 1996), i.e. YSOs surrounded by at most a moderate amount of circumstellar material. For EC 92 we find a surface gravity more similar to luminosity class III stars than to luminosity class V stars; the veiling factor is typical for infrared class II sources, i.e. PMS stars with circumstellar material.

3. K-band morphology of the SVS 4 region

In Fig. 3 we show a deep K'-band ($2.1\,\mu$m) image of the SVS 4 region, obtained for us in October 1998 by Th. Stanke with the wide-field NIR camera Omega-Prime at the Calar Alto 3.5 m telescope. This camera contains a 1024×1024 pixel HgCdTe detector and provides an image scale of $0.4''$ per pixel and a field-of-view of $6.8' \times 6.8'$. The total exposure time of this image was 10 minutes. The image is a stack of 20 exposures of 30 seconds exposure time taken at dithered positions. Each of the individual images is again a stack of 15 single exposures with 2 seconds integration time each. Clean sky exposures were constructed for each 30 second image by median averaging a number of images at different dithering positions. These sky images were subtracted from their respective science frames. Flat fielding was performed using dome flats.

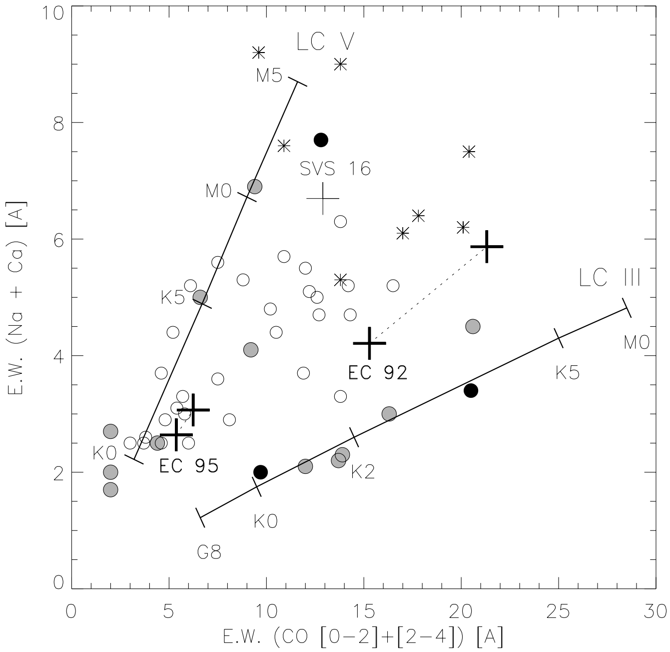

Fig. 2. Diagram of line widths, adapted from Greene & Lada (1996). The big crosses next to the labels "EC 95" and"EC 92" mark the uncorrected positions for EC 95 and EC 92 and have sizes corresponding to the uncertainties of the line widths. The crosses at the end of the connecting dotted lines mark the positions corrected for veiling. We also have included other YSOs from Greene & Lada (1996). Class I sources are shown as solid dots, flat spectrum sources as grey dots, class II sources as open circles, and class III sources as asterisks. Furthermore, we have included the infrared YSO SVS 16 in the NGC 1333 star forming region (cf. Preibisch et al. 1998), shown as a thin cross.

Aperture photometry gave magnitudes around $K \sim 18.2$ for the faintest objects in this image. Although this is 2 magnitudes below the detection limit of the Giovannetti et al. (1998) data, the image reveals no new sources within $30''$ of EC 95. The image profiles of EC 95 and EC 92 are consistent with single point-sources. Both stars are surrounded by diffuse nebulosity. No NIR counterparts can be seen for the two nearby class 0 protostars SMM 2 and SMM 4; these objects are too deeply embedded ($A_V \gtrsim 100$ mag; cf. Hurt & Barsony 1996) to be visible in the image.

4. Evolutionary status and circumstellar environment

4.1. *Location in the HR diagram*

We have used the data derived above to place EC 95 and 92 in an HR diagram and compare their positions with PMS evolutionary tracks. In Fig. 4 we have used the tracks from Siess et al. (1997). EC 95 lies very close to the $4\,M_\odot$ track at an age of 2.5×10^5 yr. The uncertainties of our data correspond to permitted ranges of $(2.2$–$4.5)\,M_\odot$ for the mass and of $(1$–$4) \times 10^5$ yr for the age of EC 95. When compared to the tracks from D'Antona & Mazz-

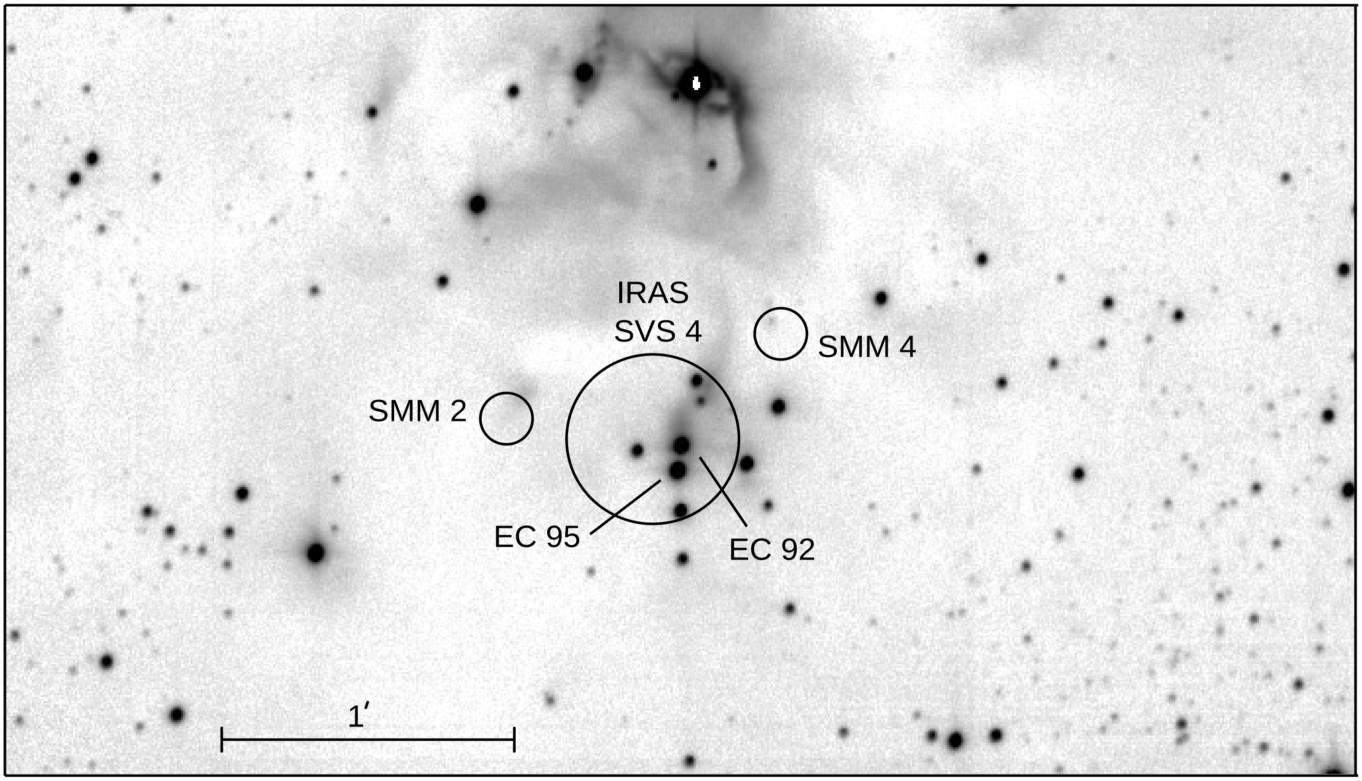

Fig. 3. Part of a deep K'-band image of the Serpens core, taken with Omega-Prime at the Calar Alto 3.5 m telescope by Th. Stanke. The field of view shown here is $4.6' \times 2.7'$. The positions of the protostellar submm sources SMM 2 and SMM 4 and the IRAS source associated with SVS 4 are marked by the circles, using the positions given by Testi & Sargent (1998) and Hurt & Barsony (1996).

itelli (1994; DM94 hereafter), EC 95 lies above the highest mass ($2.5\,M_\odot$) track of these models; its position suggests a mass of $> 2.5\,M_\odot$ and an age of $\sim 10^5$ yr. Taking the uncertainties in the stellar parameters into account, the DM94 models suggest a lower limit for the stellar mass of $> 1.5\,M_\odot$. The tracks of Swenson et al. (1994) suggest a mass of $\sim 3\,M_\odot$ (with a lower limit of $> 1.6\,M_\odot$ considering the uncertainties) and an age of $\sim 10^5$ yr. When compared to the tracks of Iben (1965), the position of EC 95 suggests the stellar mass to be in the $\sim (3–4)\,M_\odot$ range. When compared to the tracks for intermediate-mass stars from Palla & Stahler (1993), EC 95 lies slightly to the right of the birthline, where these tracks begin; however, we note that its position is again consistent with a mass of $\sim (3–4.5)\,M_\odot$. To summarize, we conclude that the best estimates for the stellar parameters of EC 95 are a mass of $\sim 4\,M_\odot$ with a conservative lower limit of $> 1.5\,M_\odot$, and an age of $\sim 2 \times 10^5$ years.

EC 92 lies above the beginning of all available tracks. We can only make a rough estimate of $\approx (0.2–0.6)\,M_\odot$ for the mass and $\lesssim 10^5$ yr for the age of this object.

In Fig. 4 we also have included the birthline[3] computed by F. Palla for an accretion rate of $10^{-4}\,M_\odot\,\mathrm{yr}^{-1}$, the data for which were kindly provided to us by F. Palla. EC 95 and 92 both lie above, but rather close to this birthline. We note that the stellar masses and ages estimated above suggest mean accretion rates of $\gtrsim 2 \times 10^{-5}\,M_\odot\,\mathrm{yr}^{-1}$ for EC 95 and of $> (2–6) \times 10^{-6}\,M_\odot\,\mathrm{yr}^{-1}$ for EC 92. Thus their positions close to the $10^{-4}\,M_\odot\,\mathrm{yr}^{-1}$ birthline appear very reasonable.

Although the uncertainties of our mass determination do not allow us to fully exclude the possibility that EC 95 might be a massive ($1.5–1.8\,M_\odot$) T Tauri star, its mass is most likely above $2\,M_\odot$. This suggest EC 95 to be a very young intermediate-mass star, which will reach the main sequence as B-type or early A-type star in a few Myr. Optically visible PMS stars in the intermediate ($1.8–10\,M_\odot$) mass range, which corresponds to spectral types B and A on the main sequence, are commonly known as Herbig Ae/Be stars. This class of stars was originally defined by Herbig (1960), who searched for the more massive analogs to T Tauri stars (cf. Herbig 1994); today, more than 200 Herbig Ae/Be stars are known (Thé et al. 1994). In its present state, EC 95 satisfies only some of the defining criteria of an Herbig Ae/Be star: it is located in a star forming region and illuminates reflection nebulosity, but it will take some 1–3 Myr until it will display a spectral type in the B–A range. Since EC 95 most likely is the extremely young progenitor of an Herbig Ae/Be star, it can be considered a “proto”- Herbig Ae/Be star.

4.2. Circumstellar material and extinction

EC 95 and 92 display very red NIR colors, but their positions in the NIR color-color diagram (see Fig. 4 in Giovannetti et

[3] The birthline is the line in the HRD where the protostars end their main accretion phase, their circumstellar envelopes get optically thin, and the YSOs become visible.

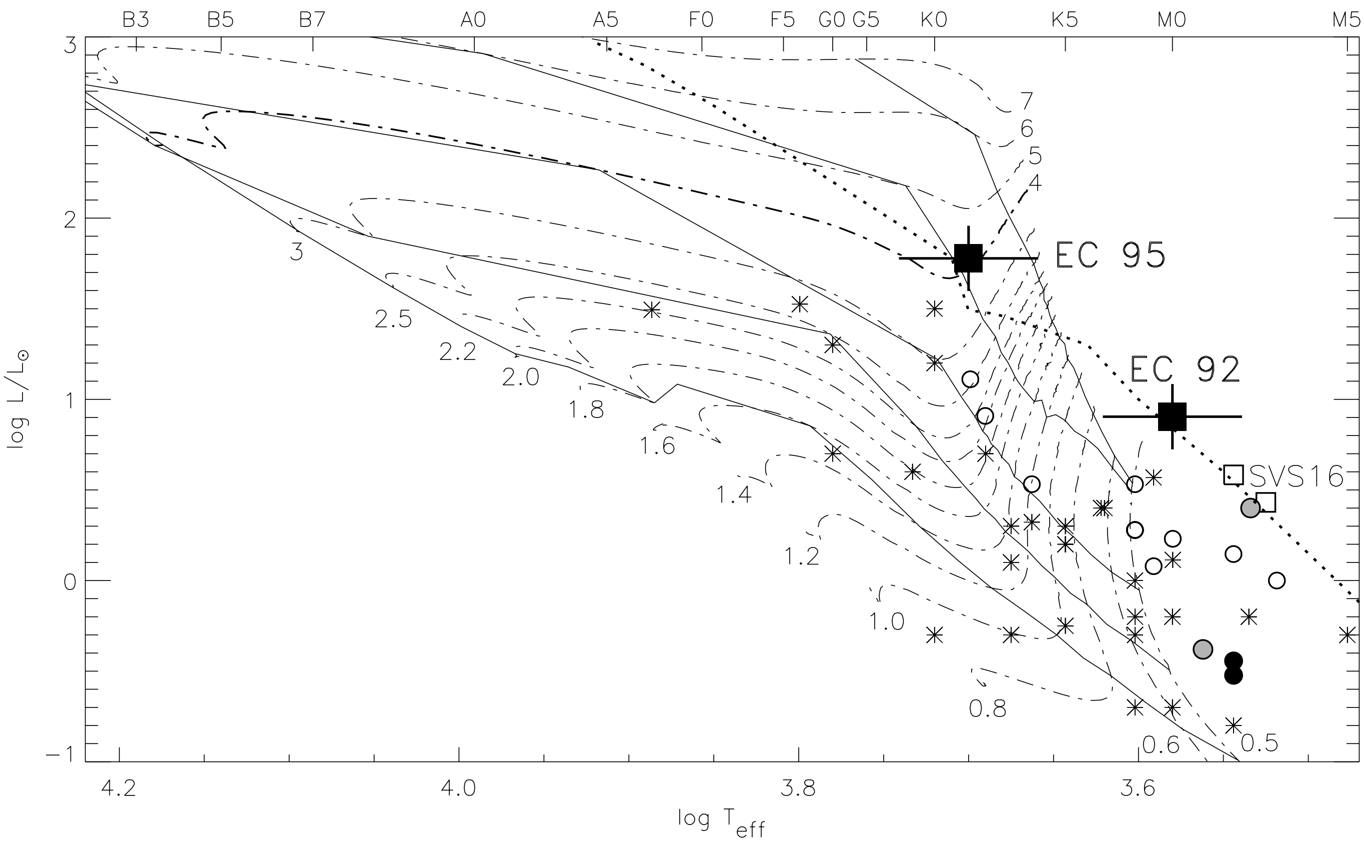

Fig. 4. HR diagram with isochrones and PMS evolutionary tracks for the "standard" $Z = 0.02$ models of Siess et al. (1997). The solid lines show the isochrones for ages of 0.1, 0.3, 1, 3, and 10 Myr. The dashed-dotted lines show evolutionary tracks which are labeled by the corresponding masses in solar units. The thick dotted line shows the birthline for low- and intermediate-mass stars computed by Palla (1998; priv. comm.) for an accretion rate of $10^{-4}\,M_\odot\,\mathrm{yr}^{-1}$. The positions for EC 95 and 92 are shown by the big solid squares with error bars. Other YSOs are from Greene & Meyer (1995), Greene & Lada (1997), and Kenyon et al. (1998). The assignment of infrared class to plot symbol is as in Fig. 2, the open squares show the very young binary SVS 16 (cf. Preibisch et al. 1998).

al. 1998) indicate only very moderate NIR excesses. This is consistent with the moderate K-band veiling factors we have found above and shows that the stars are not surrounded by large amounts of warm circumstellar material, because this would cause strong NIR excesses.

Hurt & Barsony (1996) presented high-resolution-processed IRAS images of the Serpens cloud and found a rather strong IRAS source to be associated with the SVS 4 cluster. The positional offset between EC 95 and the nominal IRAS source position is only $10''$ (see Fig. 3), but the large positional uncertainties of the IRAS data in combination with the high spatial density of YSOs do not allow a reliable identification of the IRAS source with one of the NIR sources. Thus, we can use the IRAS fluxes only as upper limits for the far-infrared fluxes of EC 95 and 92.

Testi & Sargent (1998) recently reported the results of a mm interferometric survey of the Serpens cloud core performed with the OVRO mm array. In their map, EC 95 is marginally detected at the 3σ level with a flux of 2.7 mJy, corresponding to a circumstellar mass of about $0.05\,M_\odot$. Neither EC 92 nor one of the other NIR sources within $10''$ of EC 95 is detected as a mm source. To be conservative, we will treat the 3σ detection of EC 95 as an upper limit only. The upper limit for the circumstellar mass of $\lesssim 0.05\,M_\odot$ for EC 95 is well within the typical range of circumstellar masses for class I and II YSOs of 0.002–$0.15\,M_\odot$ (André & Montmerle 1994).

In Fig. 5 we show the broadband spectral energy distributions (SEDs) of EC 95 and 92 in comparison with blackbody model SEDs for the appropriate stellar temperatures and reddening. For EC 95, the data suggest only a small excess at $2.2\,\mu$m, consistent to the small veiling found above in the spectral analysis. There is no indication for a significant excess in the 3–$10\,\mu$m range. Although we cannot exclude the possible presence of some cold circumstellar material, we conclude that EC 95 is most likely a class III source. EC 92 seems to show a moderate NIR excess and a SED typical for class II sources.

All these results indicate that the strong extinction towards EC 95 and 92 cannot be considered to be due to a dense circumstellar envelope or disk. Most likely, its is predominantly caused by interstellar extinction in the molecular cloud. This means that the stars are located deep within or behind a dense clump of the molecular cloud, probably the clump which contains the two class 0 protostars SMM 2 and SMM 4 (Hurt & Barsony 1996). The presence of such an absorbing clump can be nicely seen in

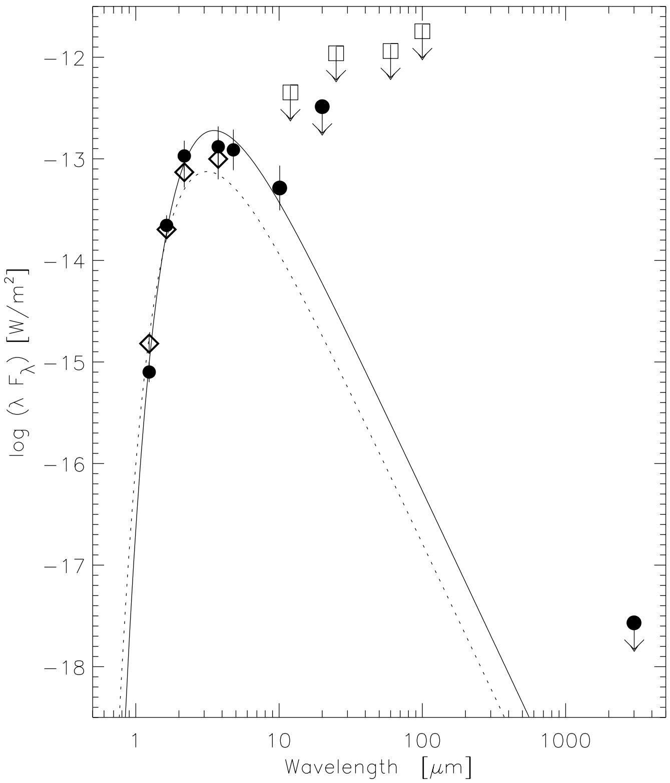

Fig. 5. Spectral energy distribution for EC 95 (solid dots) and EC 92 (open diamonds), constructed from the data in Giovannetti et al. (1998; J, H, K), Eiroa & Casali (1992; L), Gomez de Castro et al. (1988; M), and Harvey et al. (1984; N, Q). The open squares with the downward arrows mark the IRAS upper limits (Hurt & Barsony 1996). The solid and dotted lines show model SEDs constructed from blackbody models with temperature corresponding to the spectral types and with the appropriate reddening for EC 95 and 92, respectively, which have been normalized to reproduce the observed J-band fluxes.

the K-band image (Fig. 3): while one can see a large population of faint background stars with magnitudes around $K \sim 14$–16 near the edges of the image, there is a very pronounced lack of background stars in the vicinity of the SVS 4 cluster. Since the magnitude limit of this image is at about $K \sim 18$, this suggest an extinction of $A_K \gtrsim 2$–4 mag for the cloud, corresponding to $A_V \gtrsim 15$–35 mag.

4.3. Circumstellar environment and age

Since EC 95 shows no evidence for significant amounts of warm circumstellar material, and there is also no convincing evidence for a large amount of cold circumstellar matter, we conclude that EC 95 must have depleted its circumstellar material very quickly, in less than $\sim 10^5$ years. A very similar result was recently found for the YSO SVS 16 in the NGC 1333 star forming region (Preibisch et al. 1998). This dissipation time scale is very short, considering that many well studied T Tauri stars with large infrared excesses seem to be at least several 10^6 years old (e.g. Kenyon & Hartmann 1995), and indicates that the dissipation timescales can differ by orders of magnitudes for individual YSOs.

This can also be seen in the HR diagram (Fig. 4), where the YSOs of each IR class exhibit a wide range of individual ages. It is especially interesting to note that several class III YSOs are very young ($\lesssim 10^5$ yr), while the two Taurus class I sources HH 31 IRS 2 and 04489+3042, for which Kenyon et al. (1998) determined stellar parameters, appear to be much older ($\sim 10^6$ yr). This demonstrates that the evolutionary sequence of infrared classes I $\rightarrow$ II $\rightarrow$ III, which obviously must be an age sequence for individual objects, should be used with great care when trying to assign ages to YSOs according to their IR class.

5. X-ray properties

5.1. X-ray data and comparison with other YSOs

A detailed discussion of the ROSAT HRI X-ray data was given in P98. Here we only will shortly repeat the basic results. The position of the X-ray source detected in SVS 4 agrees very well with the infrared position of EC 95. Although this identification is very reliable, the formal X-ray error box also contains EC 92 and thus it cannot be fully excluded that EC 92 might be related to the X-ray source. No evidence for strong variability or flare like events could be found in the ROSAT data. Since the extinction we have determined above for EC 95 agrees well with the previous estimate used by P98 to derive the X-ray luminosity, the value of $L_{\rm X} = (1.2 \pm 0.6) \times 10^{33}$ erg/sec in the $(0.1$–$2.4)$ keV ROSAT band remains valid.

From this and the stellar parameters summarized in Table 2 we derive a fractional X-ray luminosity of $L_{\rm X}/L_{\rm bol} \sim 5 \times 10^{-3}$ and an X-ray surface flux of $F_{\rm X} \sim 1.8 \times 10^8$ $\rm erg/sec/cm^2$. These X-ray properties are very extraordinary: first, all these values are much greater than for optically visible YSOs: for the well studied class of T Tauri stars, the [median/maximum] values found for quiescent X-ray emission are $L_{\rm X} \approx [0.1/50] \times 10^{30}$ erg/sec, $L_{\rm X}/L_{\rm bol} \approx [5/30] \times 10^{-4}$, and $F_{\rm X} \approx [8/60] \times 10^6$ $\rm erg/sec/cm^2$ (see discussion in Preibisch et al. 1998). The X-ray luminosity of EC 95 is about 1000 times larger than the median value for T Tauri stars. It even exceeds the X-ray luminosity of SVS 16 in NGC 1333, which up to now appeared to be the X-ray brightest YSO (Preibisch et al. 1998), by nearly one order of magnitude.

Second, being most likely an intermediate-mass star, EC 95 is not expected to emit X-rays at all, because the two basic mechanisms for stellar X-ray emission both do not work in the intermediate mass range (e.g. Pallavicini 1989): on the one hand, these intermediate-mass stars are not expected to possess surface convection zones; thus, there should be no dynamo effect and therefore no magnetic activity which might cause X-ray emission, like observed for convective low-mass ($< 1.8\,M_\odot$) stars (including T Tauri stars). On the other hand, the intermediate-mass stars also do not have strong radiation driven stellar winds; thus the X-ray emission mechanism working in O-stars ($M > 10\,M_\odot$), where the X-rays originate in shock heated regions in the wind, cannot work either. The expectation that intermediate-mass stars should not emit X-rays, is well confirmed observationally for main sequence stars: most main sequence B- and A-stars are not detected in X-rays observations (cf. Grillo et al. 1992; Schmitt et al. 1993; Berghöfer & Schmitt 1994); the few exceptions can probably be explained by unresolved late-type companions with coronal X-ray emission.

In a noticeable contrast to these results for main sequence stars, the intermediate-mass PMS stars, i.e. the Herbig Ae/Be stars, seem to be intrinsic X-ray emitters: in ROSAT observations of about Herbig 30 Ae/Be stars, X-ray emission could be clearly detected from about half of these objects (Zinnecker & Preibisch 1994; Preibisch & Zinnecker 1996). The origin of the X-ray emission from Herbig Ae/Be stars is not yet known. Preibisch & Zinnecker (1996) discuss several possible explanations (stellar winds, companions, non-solar like dynamo models), all of which, however, face serious difficulties and cannot provide a fully satisfactory explanation.

5.2. Possible explanations for the extreme X-ray properties of EC 95

Being most likely an extremely young Herbig Ae/Be star, it is very hard to understand the X-ray properties of EC 95, since even for the much better studied optically visible Herbig Ae/Be stars the X-ray emission mechanism is not yet known. We therefore will consider different possibilities.

5.2.1. X-ray emission from a stellar wind

The high X-ray luminosities of O- and very early B-stars are generally explained by the strong and fast radiation-driven winds of these stars (cf. Pallavicini 1989; Cassinelli et al. 1994). The line-driving mechanism in these winds is inherently instable and causes strong shocks, in which the material is heated to temperatures of up to $\approx 10^6$ K (cf. Cohen et al. 1997). This X-ray emission mechanism, however, only works for very luminous stars with $L_{\rm bol} \gtrsim 10^4\,L_\odot$; observationally, there is a sharp drop in X-ray luminosities when going from B0 stars to B3 stars (Cohen et al. 1997).

We believe that the possibility of a wind related origin of the X-ray emission from EC 95 can be safely ruled out. First, EC 95 is definitely not luminous enough to generate a radiation-driven wind. Second, the very high ratio $L_{\rm X}/L_{\rm bol} \sim 5 \times 10^{-3}$ found for EC 95 is nearly five orders of magnitude greater than the typical ratios found for wind related X-ray emission from O-stars ($L_{\rm X}/L_{\rm bol} \approx 10^{-7}$; cf. Cassinelli et al. 1994).

5.2.2. X-ray emission from a low-mass companion

We cannot exclude the possibility that the X-ray radiation might originate from an unresolved low-mass companion with coronal X-ray emission. However, the typical coronal X-ray luminosities of YSOs are far (about 3 orders of magnitude) below the level we find for EC 95. Thus, this explanation would not solve, but only shift the problem of how to explain the extremely strong X-ray emission.

This case also includes the unlikely possibility that EC 92, and not EC 95, is the true X-ray source. In that case, the X-ray luminosity would be somewhat lower ($L_{\rm X} \approx 4 \times 10^{32}$ erg/sec), because the extinction towards EC 92 is lower than to EC 95. However, even this X-ray luminosity would imply a ratio $L_{\rm X}/L_{\rm bol} \sim 0.013$, much higher than typical for solar-like coronal emission from YSOs.

5.2.3. Coronal X-ray emission

Although EC 95 most likely is an intermediate-mass star and thus not expected to possess a corona, we will consider the possibility of coronal X-ray emission here. The first reason for this is that the other possibilities discussed above cannot provide us with a satisfying explanation. The second reason is that, considering the uncertainties of our mass determination above, we cannot fully exclude the possibility that the mass of EC 95 might eventually be as small as $(1.5–1.8)\,M_\odot$, i.e. that EC 95 might perhaps be a convective low-mass star.

The most useful quantity to characterize the strength of coronal X-ray emission is probably the X-ray surface flux, which ranges from about $10^4\ {\rm erg/sec/cm^2}$ for moderately active stars like the Sun to slightly more than $10^7\ {\rm erg/sec/cm^2}$ for very active stars (cf. Pallavicini 1989; Preibisch 1997). The X-ray surface flux of $F_{\rm X} \sim 1.8 \times 10^8\ {\rm erg/sec/cm^2}$ we find for EC 95 is higher than found for any other YSO and any coronally active main sequence star. However, we note that this flux level is still comparable to the maximum X-ray surface fluxes found on RS CVn stars, the most coronally active stars, which can show surface fluxes of up to $F_{\rm X} = 1.6 \times 10^8\ {\rm erg/sec/cm^2}$ (Dempsey et al. 1993). Thus, it seems possible to explain the X-ray emission from EC 95 as extremely strong coronal emission. A possible explanation for the unexpected presence of a surface magnetic field on an intermediate-mass star will be given in the next section.

6. Magnetic activity on EC 95

6.1. Radio evidence

A hint towards the presence of a surface magnetic field on EC 95 comes from radio data. Rodriguez et al. (1980) performed VLA radio observations of the Serpens cloud and could detect EC 95 at 4.9 GHz (6 cm) as an unresolved ($< 0.3''$) and rather strong source with a flux of 2.5 mJy. This corresponds to a radio luminosity of $L_{\rm 6\,cm} = 2.9 \times 10^{17}\,{\rm erg/sec/Hz}$ and is very high, when compared to other YSOs: the typical radio luminosities of YSOs are about 100 times lower, and only about 10% of the YSOs are “radio-bright”, i.e. exceed $L_{\rm 6\,cm} = 3 \times 10^{16}\,{\rm erg/sec/Hz}$ (cf. Montmerle et al. 1993). These radio-bright YSOs are thought to emit non-thermal radio radiation, which is interpreted as gyro-synchrotron radiation from electrons gyrating in the magnetic loops at the surface of these stars. Thus, the very high radio luminosity of EC 95 is another indication for the presence of a surface magnetic field.

6.2. Origin of the magnetic field

There might also be a good explanation for the presence of a surface magnetic field and a corona on EC 95: in their numerical stellar evolution calculations for intermediate-mass PMS stars, Palla & Stahler (1993) found that, during very early stages in the PMS evolution, these stars possess a surface convection zone, which is caused by subsurface deuterium burning. In their model for a $3.5\,M_\odot$ star, Palla & Stahler (1993) found the convection zone to exist for about 10^5 years. This convection zone might drive a dynamo, which could generate magnetic fields and give rise to a corona. While this very short-lived convection zone does not provide an explanation for magnetic surface activity of Herbig Ae/Be stars in general, it might be a promising explanation for the X-ray activity of the extremely young Herbig Ae/Be star EC 95.

6.3. EC 95 and the class of highly magnetized YSOs

Radio observations of several star forming regions have revealed a small population of highly magnetized diskless YSOs (André et al. 1992); about 10% of all class III YSOs seem to belong to this class. These YSOs are characterized by the following key-properties: they are “naked”, i.e. not surrounded by significant amounts of circumstellar matter, seem to be very young, are strong X-ray sources, and sources of strong non-thermal radio emission (cf. André et al. 1992; Montmerle et al. 1993). Two members of this class, DoAr 21 and HD 283447, could be spatially resolved in VLBI studies; their radio emission comes from regions with sizes of about 10 stellar radii, i.e. these stars are surrounded by very extended magnetospheres (Phillips et al. 1991).

The observed properties of this class of YSOs can probably be understood to be the consequence of their magnetospheres: the strong magnetic field might be responsible for the very quick clearing of the circumstellar matter; the lack of a circumstellar disk then implies that the magnetic coupling between the YSO and its disk, which is believed to brake the stellar rotation of YSOs (cf. Camenzind 1990; Königl 1991) cannot work for these stars. Therefore, the stellar contraction is expected to cause a strong spin-up, and the rapid stellar rotation is finally the reason for strong dynamo action and coronal activity.

Interestingly, EC 95 perfectly matches the key-properties of these magnetized diskless YSOs, and thus might well be a member of this class. It is also interesting to note that the YSO DoAr 21 in the ρ Oph star forming region, which is one of the prototypes of this class, has many very similar, although less extreme, properties than EC 95: DoAr 21 is a strongly reddened K0 star, lacking any evidence for circumstellar material. Its luminosity of $L_{\rm bol} \sim 25\,L_\odot$ suggests an age of $< 10^6$ yr, and with $L_{\rm X} \sim 2 \times 10^{31}$ erg/sec (Casanova et al. 1995) and a variable radio luminosity of about $L_{6\,\rm cm} \sim 7 \times 10^{16}\,{\rm erg/sec/Hz}$ (Phillips et al. 1991), it is one of the strongest X-ray and radio sources in the ρ Oph region. EC 95 thus might be a more massive and far more coronally active twin to DoAr 21.

7. Summary and conclusions

NIR spectroscopy of the YSO EC 95 in the Serpens molecular cloud in combination with photometric data from the literature shows this object to be an extremely young intermediate-mass star which is essentially free of circumstellar material. Probably, the only feasible explanation for the extremely strong X-ray emission of EC 95 is magnetic coronal activity, which might be caused by a dynamo working in a surface convection zone related to deuterium shell-burning. EC 95 seems to be an especially massive, very young, and extremely coronally active member of the class of young, diskless, magnetized YSOs.

It is tempting to speculate that there might be many more, still undetected, coronally very active YSOs like EC 95 or SVS 16. These objects still await to be discovered, because they are optically invisible, rather faint infrared sources which are easily confused with background stars since they lack strong infrared excesses, and their observed X-ray fluxes are very low due to the strong extinction. The new possibilities for very sensitive X-ray observations offered by the coming missions AXAF and XMM will provide us with a significantly deeper X-ray look into dense molecular cloud cores. Due to the increased sensitivity for hard ($\sim$ 3–10 keV) X-rays, which are much less affected by extinction than the softer X-rays in the ROSAT band (0.1–2.4 keV), it seems well possible to detect X-ray emission from objects suffering extinctions of more than $A_V \sim 100$ mag. This will certainly increase our knowledge about the coronal activity during extremely early phases of PMS stellar evolution.

Acknowledgements. I would like to thank Tom Geballe and the UKIRT staff for performing the spectroscopic observations of EC 95 and 92 as part of the service programme. I am also grateful to Th. Stanke, who donated some of his telescope time in order to obtain the K-band image of the Serpens core and to F. Palla for useful discussion and the data for the birthline. This work was supported by the DFG under grant Yo 5/18-2 and by a fellowship of the Max-Planck-Society. The United Kingdom Infrared Telescope is operated by the Joint Astronomy Centre on behalf of the U.K. Particle Physics and Astronomy Research Council. The ROSAT project was supported by the Bundesministerium für Bildung, Wissenschaft, Forschung und Technologie (BMBF/DLR) and the Max-Planck-Society.

References

André P., Montmerle T., 1994, ApJ 420, 837
André P., Deeney B.D., Phillips R.B., Lestrade J.-F., 1992, ApJ 401, 667
Berghöfer T.W., Schmitt J.H.M.M., 1994, A&A 292, L5
Camenzind M., 1990, In: Klare G. (ed.) Reviews in Modern Astrononmy 3, p. 234
Casanova S., Montmerle T., Feigelson E.D., André P., 1995, ApJ 439, 752
Cassinelli J.P., Cohen D.H., MacFarlane J.J., Sanders W.T., Welsh B.J., 1994, ApJ 421, 705
Cohen D.H., Cassinelli J.P., MacFarlane J.J., 1997, ApJ 487, 867
D’Antona F., Mazzitelli I., 1994, ApJS 90, 467
De Lara E., Chavarria-K. C., López Molina G., 1991, A&A 243, 139
Dempsey R.C., Linsky J.L., Flemming T.A., Schmitt J.H.M.M, 1993, ApJS 86, 599

Eiroa C. 1991, In: Reipurth B. (ed.) Low Mass Star Formation in Southern Molecular Clouds. ESO Scientific Report No. 11, p. 197
Eiroa C., Casali M.M., 1989, A&A 223, L17
Eiroa C., Casali M.M., 1992, A&A 262, 468
Giovannetti P., Caux E., Nadeau D., Monin J.-L., 1998, A&A 330, 990
Gomez de Castro A.I., Eiroa C., Lenzen R., 1988, A&A 201, 299
Greene T.P., Meyer M.R., 1995, ApJ 450, 233 (GM95)
Greene T.P., Lada C.J., 1996, AJ 112, 2184
Greene T.P., Lada C.J., 1997, AJ 114, 2157
Greene T.P., Wilking B.A., André P., Young E.T., Lada C.J., 1994, ApJ 434, 614
Grillo F., Sciortino S., Micela G., Vaiana G.S., Harnden F.R.J., 1992, ApJS 81, 795
Hartigan P., Strom K.M., Strom S.E., 1994, ApJ 427, 961
Harvey P.M., Wilking B.A., Joy M., 1984, ApJ 278, 156
Herbig G.H., 1960, ApJS 4, 337
Herbig G.H., 1994, In: Thé P.S., Pérez M.R., van den Heuvel P.J. (eds.) The Nature and Evolutionary Status of Herbig Ae/Be Stars. ASP Conf. Series Vol. 62, p. 1
Hogerheijde M.R., van Dishoeck E.F., Salverda J.M., 1999 ApJ, in press
Hurt R.L., Barsony M., 1996, ApJ 460, L45
Iben I., 1965, ApJ 141, 993
Kenyon S.J., Hartmann L., 1995, ApJS 101, 117
Kenyon S.J., Brown D.I., Tout C.A., Berlind P., 1998, AJ 115, 2491
Königl A., 1991, ApJ 370, L39
Lada C.J., 1987, In: Peimbert M., Jugaku J. (eds.) Star forming regions. IAU Symposium 115, Reidel, Dordrecht, p. 1
Montmerle T., Feigelson E.D., Bouvier J., André P., 1993, In: Levy E.H., Lunine J.I. (eds.), Protostars and planets III, University of Arizona Press, p. 689
Palla F., Stahler S.W., 1993, ApJ 418,414
Pallavicini R., 1989, A&AR 1, 177
Phillips R.B., Lonsdale C.J., Feigelson E.D., 1991, ApJ 382, 261
Preibisch Th., 1997, A&A 324,690
Preibisch Th., 1998, A&A 338, L25 (P98)
Preibisch Th., Zinnecker H., 1996, In: Zimmermann H.U., Trümper J., Yorke H.W. (eds.) Röntgenstrahlung from the Universe. MPE Report 263, p. 17
Preibisch Th., Neuhäuser R., Stanke Th., 1998, A&A 338, 923
Rieke G.H., Lebofsky M.J., 1985, ApJ 288, 618
Rodriguez L.F., Moran J.M., Ho P.T.P., Gottlieb E.W., 1980, ApJ 235, 845
Schmitt J.H.M.M., Zinnecker H., Cruddace R., Harnden F.R., 1993, ApJ 402, L13
Siess L., Forestini M., Dougados C., 1997, A&A 324, 556
Strom S.E., Vrba F., Strom K.M., 1976, AJ 81, 638
Swenson F.J., Faulkner J., Rogers F.J., Iglesias C.A., 1994, ApJ 425, 286
Testi L., Sargent A.I., 1998, ApJ 508, L91
Thé P.S., de Winter D., Pérez M.R., 1994, A&AS 104, 315
Zinnecker H., Preibisch Th., 1994, A&A 292, 152